Geldanamycin inhibits hemorrhage-induced increases in caspase-3 activity: role of inducible nitric oxide synthase

Juliann G. Kiang,[1,2] Phillip D. Bowman,[3] Xinyue Lu,[2] Yansong Li,[2] Brian W. Wu,[2] Horace H. Loh,[4] K. T. Tsen,[5] and George C. Tsokos[6]

[1]*Scientific Research Department, Armed Forces Radiobiology Research Institute, Bethesda; Departments of Radiation Biology, Medicine and of Pharmacology, Uniformed Services University of the Health Sciences, Bethesda;* [2]*Department of Cellular Injury, Walter Reed Army Institute of Research, Silver Spring, Maryland;* [3]*US Army Institute of Surgical Research, San Antonio, Texas;* [4]*Department of Pharmacology, School of Medicine, University of Minnesota, Annapolis, Minnesota;* [5]*Department of Physics and Astronomy, Arizona State University, Tempe, Arizona; and* [6]*Rheumatology Division, Beth Israel Deaconess Medical Center, Harvard Medical School, Boston, Massachussets*

Kiang JG, Bowman PD, Lu X, Li Y, Wu BW, Loh HH, Tsen KT, Tsokos GC. Geldanamycin inhibits hemorrhage-induced increases in caspase-3 activity: role of inducible nitric oxide synthase. *J Appl Physiol* 103: 1045–1055, 2007. First published May 24, 2007; doi:10.1152/japplphysiol.00100.2007.—Hemorrhage has been shown to increase inducible nitric oxide synthase (iNOS) and deplete ATP levels in tissues and geldanamycin limits both processes. Moreover, it is evident that inhibition of iNOS reduces caspase-3 and increases survival. Thus we sought to identify the molecular events responsible for the beneficial effect of geldanamycin. Hemorrhage in mice significantly increased caspase-3 activity and protein while treatment with geldanamycin significantly limited these increases. Similarly, geldanamycin inhibited increases in proteins forming the apoptosome (a complex of caspase-9, cytochrome c, and Apaf-1). Modulation of the expression of iNOS by iNOS gene transfection or siRNA treatment demonstrated that the level of iNOS correlates with caspase-3 activity. Our data indicate that geldanamycin limits caspase-3 expression and protects from organ injury by suppressing iNOS expression and apoptosome formation. Geldanamycin, therefore, may prove useful as an adjuvant in fluids used to treat patients suffering blood loss.

hemorrhagic shock; caspase-9; cytochrome c; jejunum; lung

HEMORRHAGIC SHOCK has been shown to cause systemic inflammation response syndrome, multiple organ dysfunction (MOD), and multiple organ failure (MOF; see Ref. 1). Tissue hypoxia, which frequently results from hemorrhage, has been shown to lead to acute increases in intracellular free calcium concentration ($[Ca^{2+}]_i$), 5-lipoxygenase, lipid peroxidation, cyclooxygenase, constitutive nitric oxide synthase, leukotriene B4, prostaglandin E_2, interleukin, tumor necrosis factor-α, caspases, Kruppel-like factor 6 (KLF6), inducible nitric oxide synthase (iNOS), and delayed increases in heat shock protein 70 kDa (HSP-70) and hypoxia-inducible factor-1α (6, 11, 17, 28, 30, 34, 38, 41). Investigation of the sequence of their appearance provides useful insights into the mechanisms that underlie hemorrhage-induced tissue injury and identifies therapeutic targets to prevent or reverse the injury. Experiments in iNOS-deficient mice (11), treatment of animals with iNOS inhibitors such as geldanamycin (GA; 16, 17) and 5-androstenediol (39), and information obtained from the treatment of cultured cells

with the iNOS inhibitor L-NNA (Ref. 23) suggest that iNOS-derived NO participates in the injury and the inflammatory cascade produced by hemorrhage or hypoxia.

GA is a natural product produced by *Streptomyces hygroscopicus* that binds with high affinity to the ATP binding pocket of heat shock protein 90 kDa (HSP-90). We reported that GA upregulates inducible HSP-70 (HSP-70i) and downregulates HSP-90 (17). It protects mice (16) and rats (34) from hemorrhage-associated organ damage by inhibiting iNOS expression. The GA-induced upregulation of HSP-70i preserves pyruvate dehydrogenase and ATP (16). The ability of GA to downregulate HSP-90 is the basis for current medical protocols attempting to manage solid tumors and lymphoma (http://clinicaltrials.gov/ct/show/NCT00248521).

Caspase-3 is an aspartate-specific cystenyl protease that plays a key role in activating many downstream caspases involved in apoptosis (13, 14, 22, 25). Hemorrhage increases caspase-3 cellular activity (5, 18, 26, 27, 29, 31, 45) and decreases cellular ATP levels in various tissues (16, 19, 24, 32–34, 43). Agents that increase HSP-70i and inhibit iNOS have been shown to ameliorate hemorrhage-induced cell injury (17, 19, 34). However, the relationship between iNOS and caspase-3 remains unclear. In this study, we examined the mechanisms whereby GA confers tissue protection in mice subjected to hemorrhage. We are the first to report a time course study of caspase-3 after hemorrhage. Treatment with GA limits the hemorrhage-induced increase in caspase-3 protein and activity by limiting the expression of iNOS and apoptosome formation in the cytosol.

METHODS

Research was conducted in compliance with the Animal Welfare Act and other federal statutes and regulations relating to animals and experiments involving animals and adheres to principles stated in the *Guide for the Care and Use of Laboratory Animals*, NRC Publication, 1996 edition. The animal protocol was reviewed and approved by Institutional Animal Care and Use Committee at US Army Institute of Surgical Research.

Animal protocols. Experiments were conducted using the mouse model described by Song et al. (40). Male Swiss Webster mice weighing 25–35 g were briefly anesthetized with isoflurane, and 40%

Report Documentation Page

1. REPORT DATE	2. REPORT TYPE	3. DATES COVERED
01 SEP 2007	**N/A**	**-**

4. TITLE AND SUBTITLE	5a. CONTRACT NUMBER
Geldanamycin inhibits hemorrhage-induced increases in caspase-3 activity: role of inducible nitric oxide synthase	5b. GRANT NUMBER
	5c. PROGRAM ELEMENT NUMBER

6. AUTHOR(S)	5d. PROJECT NUMBER
Kiang J. G., Bowman P. D., Lu X., Li Y., Wu B. W., Loh H. H., Tsen K. T., Tsokos G. C.,	5e. TASK NUMBER
	5f. WORK UNIT NUMBER

7. PERFORMING ORGANIZATION NAME(S) AND ADDRESS(ES)	8. PERFORMING ORGANIZATION REPORT NUMBER
United States Army Institute of Surgical Research, JBSA Fort Sam Houston, TX 78234	

9. SPONSORING/MONITORING AGENCY NAME(S) AND ADDRESS(ES)	10. SPONSOR/MONITOR'S ACRONYM(S)
	11. SPONSOR/MONITOR'S REPORT NUMBER(S)

12. DISTRIBUTION/AVAILABILITY STATEMENT
Approved for public release, distribution unlimited

13. SUPPLEMENTARY NOTES

14. ABSTRACT

15. SUBJECT TERMS

16. SECURITY CLASSIFICATION OF:			17. LIMITATION OF ABSTRACT	18. NUMBER OF PAGES	19a. NAME OF RESPONSIBLE PERSON
a. REPORT **unclassified**	b. ABSTRACT **unclassified**	c. THIS PAGE **unclassified**	**SAR**	**11**	

of the calculated blood volume was removed over a 1-min period by cardiac puncture with a 26-gauge needle. Mean arterial blood pressure fell from 80 to 40 mmHg in the 2 h following treatment. Treated mice were allowed to respond for 1, 3, 6, 12, 24, and 48 h. Sham-treated animals underwent cardiac puncture, but no blood was removed.

Geldanamycin treatment. GA was obtained from Sigma-Aldrich Chemical (St. Louise, MO). In different experiments, mice were pretreated with 10% DMSO saline or GA (1 μg/g body wt) in 10% DMSO saline by intraperitoneal injection 16 h before hemorrhage (34).

These mice were then subjected to 40% hemorrhage and allowed to respond for 6 h before they were killed. A small portion of lung, jejunum, kidney, heart, brain, and liver was removed from the treated mice and frozen immediately at −70°C until used for immunoblotting and biochemical assays. Another set of these tissues was used for histology examination.

Tissues were minced, sonicated for 15 s, and then centrifuged at 10,000 *g* for 10 min. The supernatant was saved for determining the total amount of protein in each lysate sample and performing immunoblot analysis. The caspase-3 cellular activity was measured. Proteins and moieties were assessed by immunoprecipitation and immunoblotting using antibodies for caspase-3, cytochrome c, and Apaf-1.

Histopathologic assessment. Small intestine tissue specimens were rinsed in cold saline solution and immediately fixed in 10% buffered formalin phosphate. The tissue was then embedded in paraffin, sectioned transversely, and stained with hemotoxylin and eosin. The mucosal damage of jejunum for each slide was graded on a six-tiered scale defined by Chiu et al. (4) as follows: grade 0, normal mucosa; grade 1, development of subepithelial spaces near the tips of the villi with capillary congestion; grade 2, extension of the subepithelial space with moderate epithelial lifting from the lamina propria; grade 3, significant epithelial lifting along the length of the villi with a few denuded villus tips; grade 4, denuded villi with exposed lamina propria and dilated capillaries; and grade 5, disintegration of the lamina propria, hemorrhage, and ulceration. Lung tissues for histopathological assessment were prepared in the same manner as small intestine; alveolar wall thickness was measured.

Cell culture. Human intestinal epithelial T84 cells, FHs74 Int cells, and CRL-1550 cells (American Type Cell Culture, Rockville, MD) were grown in Dulbecco's modified Eagle medium (DMEM), hybridcare medium, and RPMI 1640, respectively, in a humidified incubator with a 5% CO_2 atmosphere. Each medium was supplemented with 2 mM glutamine, 4.5 gm/l glucose, 10% fetal bovine serum, 100 U/ml penicillin, and 100 μg/ml streptomycin, pH 7.4 (Quality Biological, Gaithersburg, MD). Cells were fed every 3–4 days. Cell viability was determined by the trypan blue exclusion assay. Twenty microliters of cell suspension was mixed with 20 μl of 0.4% trypan blue solution (Sigma Chemical, St. Louis, MO). Viability was calculated accordingly.

iNOS gene construct. iNOS gene was used in this study. cDNA of human iNOS was obtained from Dr. N. Tony Eissa (Baylor College of Medicine, Houston, TX; Ref. 10). A 3362-bp coding sequence with *Hind* III and *Xho* I restriction sites at each terminus of human iNOS gene was subcloned from this full length of human iNOS cDNA. For PCR, we used the forward and reverse primers, 5′-CT AAG CTT GTC ATG GCC TGT CCT TGG AAA TTT CTG TTC-3′ and 5′-GAC TCG AGC TCA GAG CGC TGA CAT CTC CAG GCT-3′, respectively. After digestion and purification of the PCR amplification product, the expression cDNA sequence was used for insertion into the vector. The vector used in this study was pcDNA3.1 (Invitrogen, San Diego, CA). The expression cDNA of iNOS gene was inserted between the *Hind* III and *Xho* I sites of pcDNA 3.1 vector. The expression construct then was sequenced to confirm its correct sequence and open reading frame.

Transient gene transfection. Cells were cultured in six-well plates (1.5 × 10⁶ cells/well). Cells in each well were treated with 4 μg iNOS expression plasmid in 0.5 ml antibiotics-free growth medium using a Lipofectamine 2000 transfection kit (Invitrogen, Carlsbad, CA) and the manufacturer's protocol. Control cells were treated with blank pcDNA 3.1 vector. DMEM (1.5 ml) was then added to each well, and the cells were returned to the incubator for 24 h to allow transient transfection.

iNOS small interfering RNA transfection. RNA interference technology was used to decrease iNOS protein levels. Two designed pairs of oligoduplexes targeted against iNOS were purchased from Qiagen (Valencia, CA). The target sequences of the oligoduplexes are the NOS-S sense strand, 5′-ACAACAGGAACCUACCAGCTT-3′, and NOS-AS antisense strand, 5′-GCUGGUAGGUUCCUGUUGUTT-3′, respectively. A nonspecific oligoduplex (nonsilencing control, targeting AAU UCU CCG AAC GUG UCA CGU) at the same final concentrations as the iNOS RNA duplexes was used as a negative control. To maximize siRNA silencing potential, small interfering RNAs (siRNAs) were heated for 1 min at 90°C, followed by 60 min at 37°C before the siRNA transfection. Prior to transfection, cells were grown in fresh medium without antibiotics for 24 h. Cells were then transferred to six-well plates (2 × 10⁶ cells/well). The transient transfection with siRNA duplexes at 100 nM was performed using the Lipofectamine reagent (Invitrogen). Twenty-four hours after transfection, cells were either exposed to 10 mM NaCN or vehicle (saline) for 1 h to allow hypoxia to occur. Cells were allowed to recover in the incubator for 23 h before harvesting and analysis.

Immunoprecipitation. Tissue lysates containing 300 μg protein were incubated with the antibody for caspase-9 or cytochrome c (5 μl), chilled on ice for 1 h, mixed with protein A/G agarose beads (50 μl; Santa Cruz Biotechnology, CA), and incubated overnight on a nutator at 4°C. The immunoprecipitate was collected by centrifugation at 12,500 *g* for 10 min, washed twice with 500 μl of stop buffer and once with 500 μl PBS wash buffer. The pellet was resuspended in 50 μl of electrophoresis sample buffer without 2-mercaptoethanol, boiled for 5 min, and then centrifuged for 30 s to remove the agarose beads. The supernatant was incubated with 5% 2-mercaptoethanol at 37°C for 1 h. Twenty-five microliters of sample was loaded onto precast 10% Tris-glycine polyacrylamide gels for Western blots.

Western blots. Twenty micrograms of each sample was resolved on SDS-polyacrylamide slab gels (precast 10% gels; Invitrogen, Carlsbad, CA). Protein was then blotted onto a nitrocellulose membrane (type NC, 0.45 μm; Schleicher and Schuell) using a Novex blotting apparatus and the manufacturer's protocol. The nitrocellulose membrane was blocked by incubation for 90 min at room temperature in Tris-buffered saline containing 0.1% Tween 20 (TBST) and 3% nonfat dried milk. The blot was then incubated for 60 min at room temperature with antibodies against actin (Santa Cruz Biotechnology), active caspase-3 and caspase-9 (Epitomics, Belmont, CA), cytochrome c (Upstate, Lake Placid, NY), and Apaf-1 (GeneTex, TX) at 1 μg/ml in TBST with 3% nonfat dried milk. The blot was washed three times (10 min each) in TBST before incubating for 60 min at room temperature with a 1,000× dilution of species-specific IgG peroxidase conjugate (Santa Cruz Biotechnology) in TBST with 3% nonfat dried milk. The blot was washed six times (5 min each) in TBST before detection of the peroxidase activity using the Enhanced Chemiluminescence kit (Amersham Life Science Products, Arlington Heights, IL).

Measurements of caspase-3 activity. Caspase-3 activity was determined using the CASPASE-3 Cellular Activity Assay Kit PLUS (Biomol, Plymouth Meeting, PA). In brief, 10 μl of each sample lysate was added to wells of a 96-well plate already containing the substrate Ac-Asp-Glu-Val-Asp-pNitroaniliane (Ac-DEVD-pNA). Caspase in the lysates cleaved the substrate to pNA as indicated by an increase in absorbance at 405 nm, which was used to determine reaction rate. Absorbance was measured using a SpectraMax 250 spectrophotometric plate reader and SOFTmax Pro 3.1.1 software (Molecular Devices, San Diego, CA). Data were normalized to total protein, and caspase-3 activity was expressed as picomoles pNA per minute per microgram of protein.

Immunofluorescent staining for confocal microscopy. Cells (1 × 10⁵) were plated on a glass coverslip precoated with poly-L-lysine. After attachment, the cells were fixed with 3.7% formaldehyde and permeabilized with 0.1% Triton X-100 in PBS for 10 min. The permeabilized cells were blocked with 2% BSA for 30 min and then incubated for 1 h with a rabbit anti-human caspase-9 monoclonal antibody (1:200 dilution; Epitomics) and a mouse anti-human cytochrome c monoclonal antibody (Upstate) at a 1:200 dilution in PBS containing 2% BSA. The cells were then incubated for 1 h with Alexa Fluor 488 goat anti-mouse IgG (1:400 dilution; Molecular Probes) and Alexa Fluor 594 goat anti-rabbit IgG (1:400 dilution; Molecular Probes). Cells were washed three times with PBS between each step. After staining with antibodies, the cells were mounted on a glass slide using the SlowFade light antifade kit with 4′,6-diamidino-2-phenylindole (Molecular Probes) and inspected microscopically under a laser confocal scanning microscope.

Solutions. Na⁺ Hanks' solution contained (in mM): 145 NaCl, 4.5 KCl, 1.3 $MgCl_2$, 1.6 $CaCl_2$, and 10 HEPES (pH 7.40 at 24°C). Na⁺ Hanks' stop buffer contained (in mM): 50 Tris·HCl, 1% NP-40, 0.25% Na⁺-deoxycholate, 150 NaCl, 1 EDTA, 1 phenylmethanesulfonyl fluoride, 1 Na_3VO_4, 1 NaF, along with aprotinin, leupeptin, and pepstatin (10 µg/ml each). Na⁺ Hanks' wash buffer contained (in mM): 1 EDTA, 1 phenylmethanesulfonyl fluoride, 1 DTT, 1 Na_3VO_4, 1 NaF, along with aprotinin, leupeptin, and pepstatin (10 µg/ml each).

Statistical analysis. All data are expressed as mean ± SE. One-way ANOVA, two-way ANOVA, Studentized-range test, Bonferroni's inequality, and Student's *t*-test were used for comparison of groups with 5% as a significant level.

RESULTS

Hemorrhage increases caspase-3 activity in mouse organs. We performed experiments to determine the time course of the hemorrhage-associated increase in caspase-3 activity in selected tissues (see Ref. 19; Fig. 1). In jejunum and lung, caspase-3 activity increased within the first hour but then decreased to levels below baseline at 3 h before increasing once again. In jejunum, the increase in caspase-3 activity after 3 h persisted until 12 h before returning to baseline levels at 24 and 48 h (Fig. 1*A*). In lung, the increased activity after 3 h reached a plateau at 6 h that was maintained (Fig. 1*B*). In heart, caspase-3 activity increased after 3 h, peaked at 6 h, and then returned to baseline by 12 h (Fig. 1*C*). In kidney, the activity
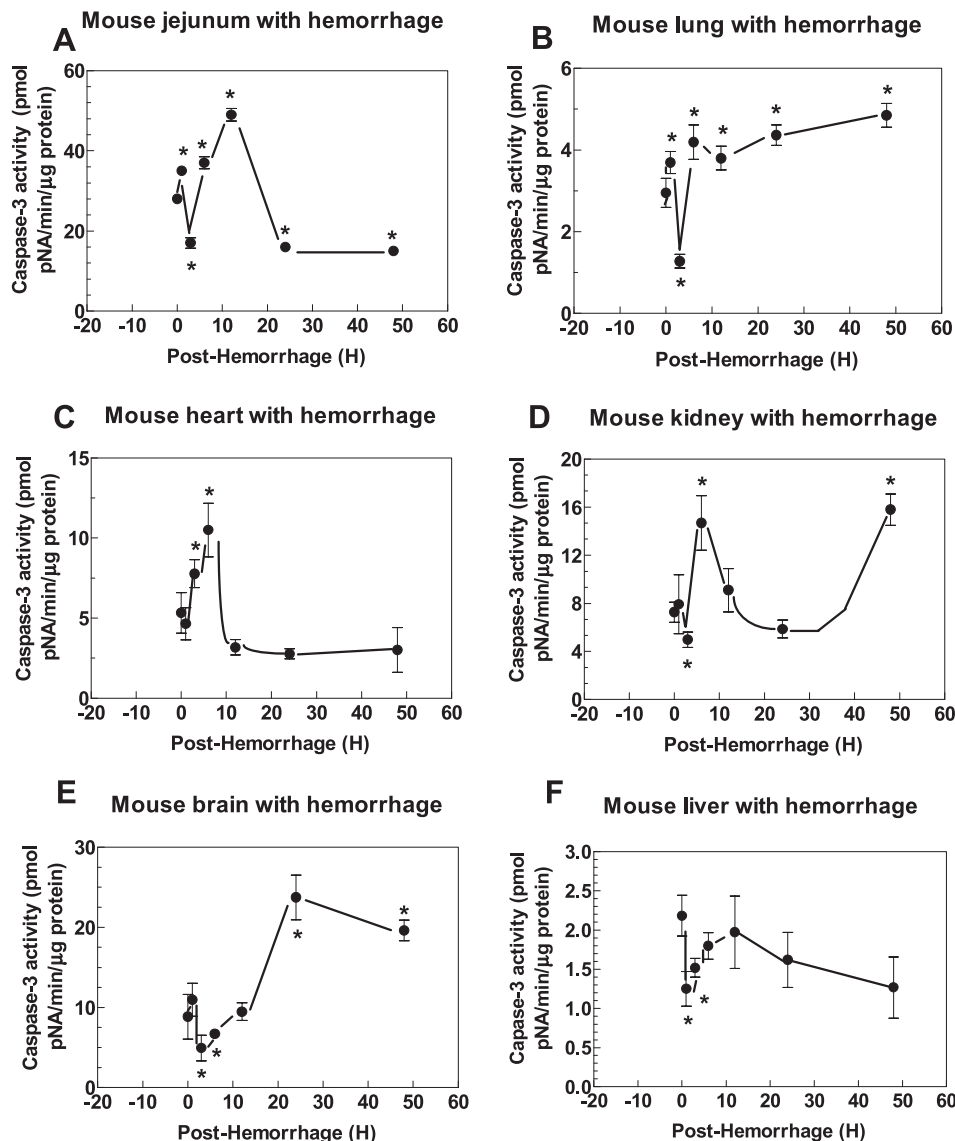

Fig. 1. Time course of caspase-3 activity in lysates of organs of mice subjected to hemorrhage. Mice were exposed to hemorrhage and allowed to respond for 1, 3, 6, 12, 24, or 48 h (*n* = 6). Caspase-3 activity was measured in lysates of jejunum, lung, heart, kidney, brain, and liver. Data collected from hemorrhaged organs were compared with those from sham-operated organs. *$P < 0.05$ vs. *t* = 0 h, determined by Student's *t*-test.

was decreased by 3 h but increased and peaked at 6 h before returning to baseline at 24 h; however, it reached another peak at 48 h (Fig. 1D). In contrast, brain caspase-3 activity decreased steadily until 6 h but increased at 24 h and remained at high levels at 48 h (Fig. 1E). Unlike the jejunum, lung, heart, brain, and kidney, liver caspase-3 activity decreased within the first 3 h after hemorrhage before returning to baseline by 12 h (Fig. 1F).

Treatment with GA inhibits hemorrhage-induced increase in caspase-3 in mouse organs. We treated mice by intraperitoneal injection with GA 16 h before subjecting them to hemorrhage. Caspase-3 activity in various tissues was measured 6 h later. Figure 2 shows that treatment with GA significantly blocked caspase-3 activity in jejunum (Fig. 2A), lung (Fig. 2B), heart (Fig. 2C), and kidney (Fig. 2D). GA did not affect caspase-3 activity in brain and liver tissues at this time point (Fig. 2, E and F).

Hemorrhage increases caspase-3 protein in the jejunum. To determine whether increases in caspase-3 activity were associated with increased amounts of caspase-3 protein, we blotted jejunum tissue lysates from animals 6 h after hemorrhage. Figure 3 (lane 2) demonstrates that hemorrhage caused a significant increase in caspase-3 protein. Since GA treatment

was shown above to prevent the hemorrhage-induced increase in caspase-3 activity, we asked whether treatment with GA prevented increases in caspase-3 protein expression. Indeed, GA prevented the hemorrhage-induced increase in caspase-3 protein in jejunum tissue lysates (Fig. 3, lane 4), whereas GA alone elevated the basal level of caspase-3 protein (Fig. 3, lane 3). The results suggest that the increased caspase-3 activity results from increased caspase-3 protein expression.

GA inhibits the hemorrhage-induced formation of apoptosomes in jejunum tissue. The apoptosome is an aggregation of caspase-9, cytochrome c, and Apaf-1 and is known to activate caspase-3 (13, 14, 22, 25). We sought to determine if an increase in apoptosomes is responsible for the upregulation of caspase-3 protein that causes the increase in cellular caspase-3 activity observed after hemorrhage. We performed immunoprecipitation experiments followed by immunoblotting to measure changes in apoptosome proteins following hemorrhage and to determine the effect of GA treatment on their formation. When jejunum tissue lysates were immunoprecipitated with anti-caspase-9 antibody and the precipitates were blotted with anti-cytochrome c or anti-Apaf-1 antibodies, bands corresponding to cytochrome c (Fig. 4A) and Apaf-1 (Fig. 4B) were detected. When the lysates were immunoprecipitated with
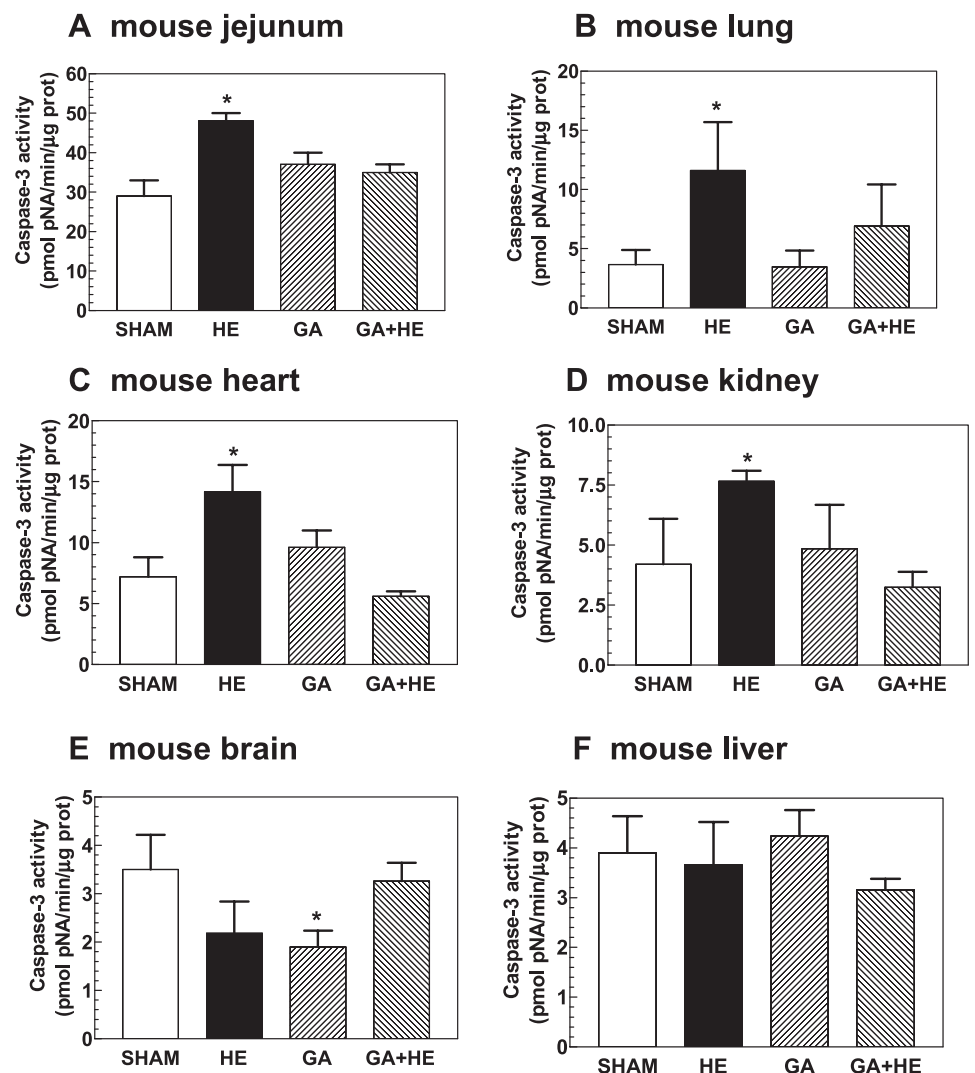

Fig. 2. Geldanamycin (GA) inhibits hemorrhage-induced increase in caspase-3 activity in mouse organs. Mice were treated with GA or 10% DMSO saline by intraperitoneal injection 16 h before hemorrhage (HE; $n = 6$). Caspase-3 activity was measured in lysates of jejunum, lung, heart, kidney, brain, and liver. $*P < 0.05$ vs. Sham, GA, and GA+HE for jejunum, lung, heart, and kidney; $*P < 0.05$ vs. Sham and GA+HE for brain, determined by χ^2 test.
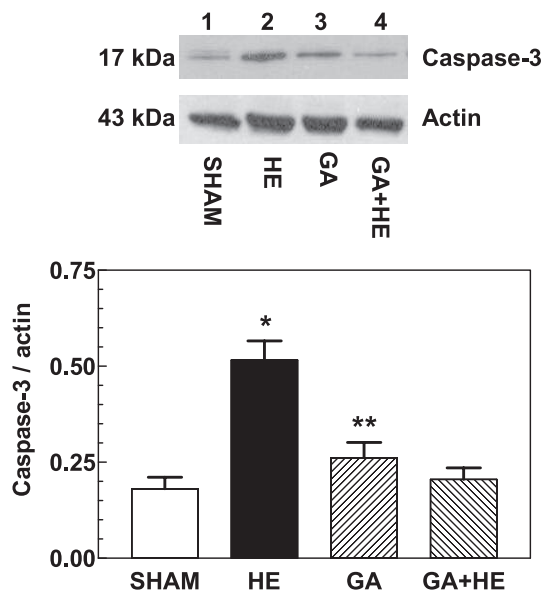
Fig. 3. GA limits the hemorrhage-induced increases in caspase-3 protein. Mice were pretreated with GA or 10% DMSO saline by intraperitoneal injection 16 h before HE ($n = 6$). Caspase-3 protein in lysates of jejunum was measured by immunoblot analysis. The caspase-3 protein band was quantitated densitometrically and normalized to actin. *$P < 0.05$ vs. Sham, GA, and GA+HE; **$P < 0.05$ vs. Sham, HE, and GA+HE, determined by χ^2 test.

anti-cytochrome c antibody and precipitates were blotted with anti-caspase-9 and anti-Apaf-1 antibodies, caspase-9 (Fig. 4C) and Apaf-1 bands (Fig. 4D) were detected. The intensity of cytochrome c (Fig. 4A, lane 3), Apaf-1 (Fig. 4, B and D, lane 3), and caspase-9 (Fig. 4C, lane 3) was greater than that from the sham-treated lysates (Fig. 4, A–D, lane 2). Treatment with GA alone did not affect the expression of these proteins (Fig. 4, A–D, lane 4), whereas it decreased (Fig. 4, A–D, lane 5) the hemorrhage-induced increases in the expression of all studied proteins. Taken together, these data indicate that hemorrhage increases the expression of protein members of the apoptosome and GA prevents that increase.

GA increases survival from hemorrhagic shock and prevents hemorrhage-induced organ injury. We previously reported that 6 h after hemorrhage 60% of mice survive (16). Mice treated with GA survived hemorrhage at higher rates (84%). Histologic assessment of the mouse jejunum and lung tissue showed that hemorrhage reduced the villus height and increased the villus width in jejunum with no alteration of crypt depth (Fig. 5B). The mucosal damage grade of hemorrhaged jejunum tissue was 3.0 ± 0.52 (Fig. 5E, $P < 0.05$ vs. Sham). Hemorrhage also caused a thickening of the alveolar wall (Fig. 5, B and F).

GA treatment alone did not alter villus height and width or the crypt depth (Fig. 5C). However, GA treatment prior to hemorrhage protected jejunum (Fig. 5D), and the mucosal damage grade was reduced to the level recorded in sham-treated animals (Fig. 5E). Likewise, GA treatment limited pulmonary injury (Fig. 5D), and the thickness of the alveolar wall remained the same as that in lung of the sham-treated mice (Fig. 5F).

Hypoxia-induced increase in caspase-3 depends on iNOS but not Ca^{2+} and PI3K/Akt. It is known that hypoxia, a model of hemorrhage in animal, increases $[Ca^{2+}]_i$, which results from

increased Ca^{2+} influx followed by an elevated Ca^{2+} mobilization (21). To determine whether the hypoxia-induced increase in caspase-3 correlated with increased $[Ca^{2+}]_i$, cultured intestinal epithelial cells were exposed to hypoxia in Ca^{2+}-free buffer containing 3 mM EGTA. Removal of external Ca^{2+} failed to inhibit the hypoxia-induced increase in caspase-3 (Fig. 6A). Both N$^\omega$-nitro-L-arginine (L-NNA) and L-N^6-(1-iminoethyl)lysine (L-NIL) (iNOS inhibitors) were capable of blocking the increase (Fig. 6B), suggesting a relationship between increases in caspase-3 and iNOS observed in cells exposed to hypoxia.

The increase in caspase-3 is known to be mediated by the PI3K/Akt pathway. However, treatment with LY-29402 (a known
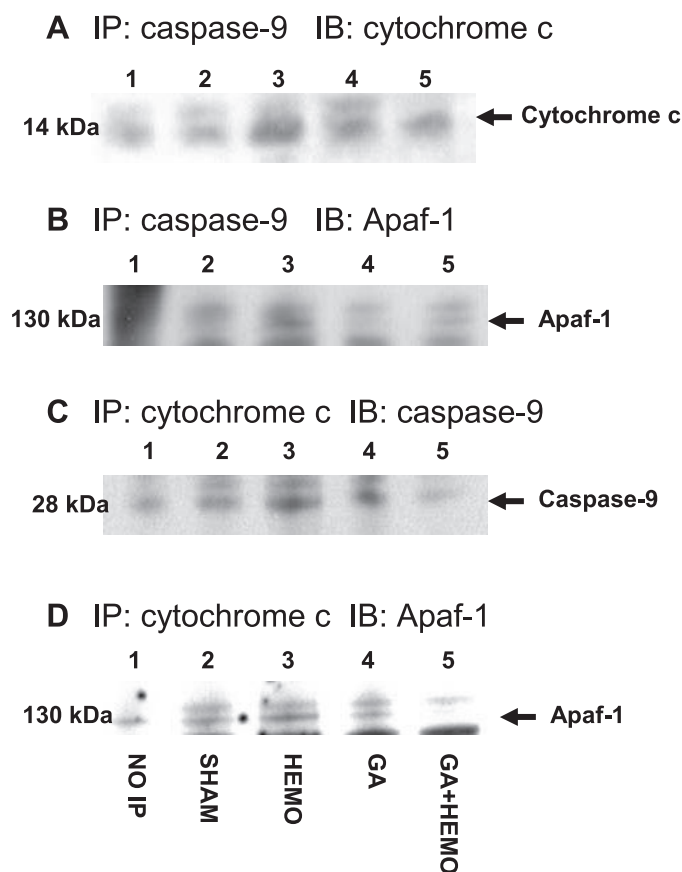

Fig. 4. Hemorrhage-induced increases in cytochrome c lead to formation of complexes with caspase-9 and Apaf-1; GA prevents formation. Mice were pretreated with GA or 10% DMSO saline by intraperitoneal injection 16 h before hemorrhage ($n = 6$). A: representative Western blot of jejunum cytochrome c complex formation with caspase-9. Lysates of mouse jejunum were immunoprecipitated (IP) with anti-caspase-9 antibody, and cytochrome c was then detected with anti-cytochrome c antibody using immunoblot (IB) analysis. B: representative Western blot of jejunum Apaf-1 complex formation with caspase-9. Lysates of mouse jejunum were IP with anti-caspase-9 antibody, and Apaf-1 was then detected with anti-Apaf-1 antibody using IB analysis. C: representative Western blot of jejunum cytochrome c complex formation with caspase-9. Lysates of mouse jejunum were IP with anti-cytochrome c antibody, and caspase-3 was then detected with anti-caspase-9 antibody using IB analysis. D: representative Western blot of jejunum cytochrome c complex formation with Apaf-1. Lysates of mouse jejunum were IP with anti-cytochrome c antibody, and Apaf-1 was then detected with anti-Apaf-1 antibody using IB analysis. Previous assessments (data not shown) have shown efficiency of IP to be constant. *Lane 1*: no IP (normal mouse serum used instead of antibody); *Lane 2*: Sham, mouse received same handling and procedures as hemorrhaged mouse but no hemorrhage; *Lane 3*: HEMO, hemorrhage; *Lane 4*: GA; *Lane 5*: GA+HEMO, GA given before hemorrhage.
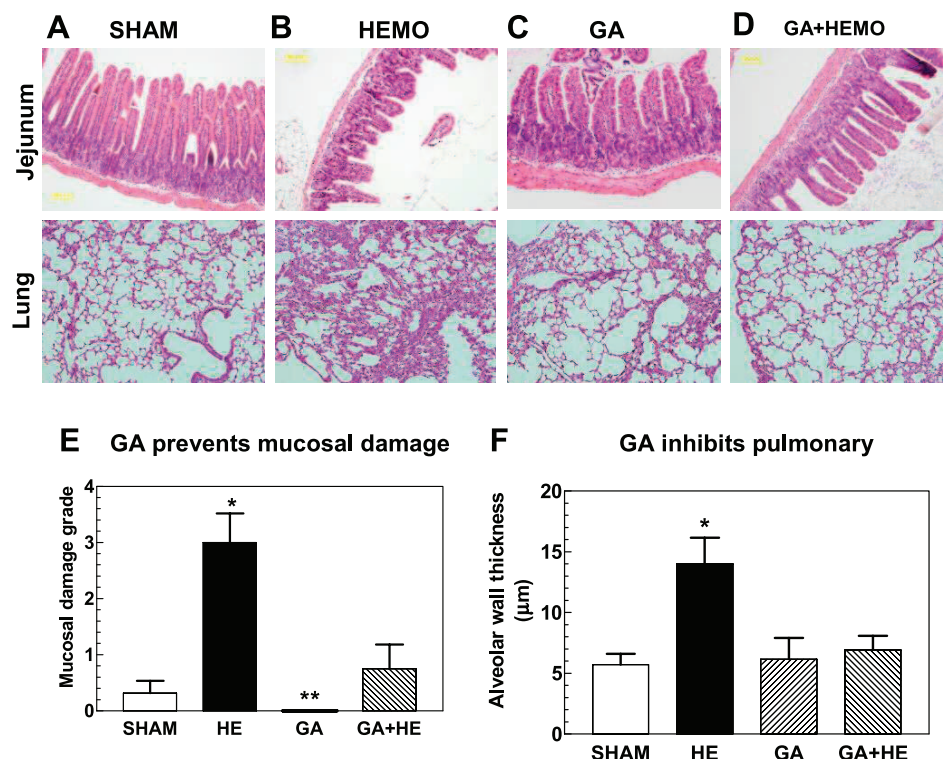
Fig. 5. GA prevents hemorrhage-induced tissue damage in jejunum and lung. Low-power photomicrographs of full-thickness sections of jejunum in sham treated (*A*), subjected to hemorrhage (*B*), GA treated (*C*), and GA treated before hemorrhage (*D*). Histological severity of injury grade for jejunum tissue section is: Sham, 0.32 ± 0.22; HEMO, 3.0 ± 0.52; GA, 0; and GA+HEMO, 0.75 ± 0.43. Histological severity of alveolar thickness for lung tissue section is: Sham, 5.7 ± 0.9; HEMO, 14 ± 2.2; GA, 6.2 ± 1.8; and GA+HEMO, 6.9 ± 1.2. *$P < 0.05$ vs. Sham, GA, and GA+HE, **$P < 0.05$ vs. Sham, HE, and GA+HE, determined by χ^2 test.

inhibitor of PI3K/Akt pathway) did not attenuate the caspase-3 response to hypoxia (Fig. 6*C*), whereas treatment with a DEVD inhibitor (a specific inhibitor of caspase-3) effectively diminished the response (Fig. 6*D*), suggesting the presence of a pathway different from the known PI3K/Akt.

We reported that iNOS protein is positively correlated with caspase-3 enzymatic activity (20). In these experiments we sought to test whether there is a correlation between iNOS and caspase-3 protein levels. Intestinal epithelial cells were used to study the correlation between iNOS and caspase-3 because the injury was observed on villi (Fig. 5*B*). The level of iNOS protein in the cell was increased by iNOS gene transfection or exposure to hypoxia and decreased by treatment with iNOS siRNA. The amount of caspase-3 protein was also determined after each of these treatments. Caspase-3 protein was greatly upregulated in cells overexpressing iNOS, whereas the cells transfected with the empty vector exhibited a significant yet much lower increased level of caspase-3 protein (Fig. 7*A*). Hypoxia significantly increased caspase-3 protein that was inhibited by transfer of iNOS siRNA into cells (Fig. 7*B*). Treatment with iNOS siRNA alone did not alter the basal level of caspase-3. Caspase-3 enzymatic activity in iNOS gene-transfected cells increased by $230 \pm 25\%$ ($n = 6$, $P < 0.05$ vs. control and empty vector) and failed to increase in iNOS siRNA-treated cells.

iNOS increases apoptosome formation. Next we determined whether iNOS influences the formation of apoptosome, thereby leading to changes in caspase-3 activity. Using confocal microscopy we demonstrated that iNOS gene transfection (Fig. 8) resulted in increased cytochrome c in cytoplasm that colocalized with caspase-9. Images of cells exposed to hypoxia displayed a similar result (Fig. 9). Transfer of iNOS siRNA into cells blocked the hypoxia-induced colocalization of cyto-

chrome c and caspase 9 (Fig. 9). The results suggest that the level of iNOS is related to apoptosome formation that triggers caspase-3 activity.

DISCUSSION

Hemorrhagic shock is known to cause MOD and MOF (1, 15). There remain no effective treatments for the potentially lethal health effects that result from hemorrhage. The effort to develop effective treatments will greatly benefit from a better understanding of the mechanisms involved. Numerous cell signaling ions and molecules are known to play roles in the pathology of hemorrhage (6, 11, 15, 17–19, 28, 30, 34, 38, 41). They include among others, ATP levels, transcription factors, and apoptotic proteins such as caspase-3.

In the present study we showed that hemorrhage increased caspase-3 activity in jejunum, lung, heart, kidney, and brain tissue lysates (Fig. 1, *A*–*E*). These data represent the first time course reported for the caspase-3 response after hemorrhage. As the data show, the response is complex and varies with tissue type. In general, caspase-3 activity increased in all tissues examined except liver. Activity in jejunum and heart tissues returned to basal levels within 24 h; whereas activity in lung, kidney, and brain remained above basal levels for at least 48 h after treatment.

We sought to determine the effect of GA on the hemorrhage-induced increase in caspase-3 activity. GA has been shown to block several cell-signaling molecules involved in the response to hemorrhage, and it improves survival of mice subjected to hemorrhage injury (16, 34). Figure 2 demonstrates that GA blocks the hemorrhage-induced increases in caspase-3 activity in all tissues in which an increase was observed. The variable degree of inhibition observed after GA treatment may reflect
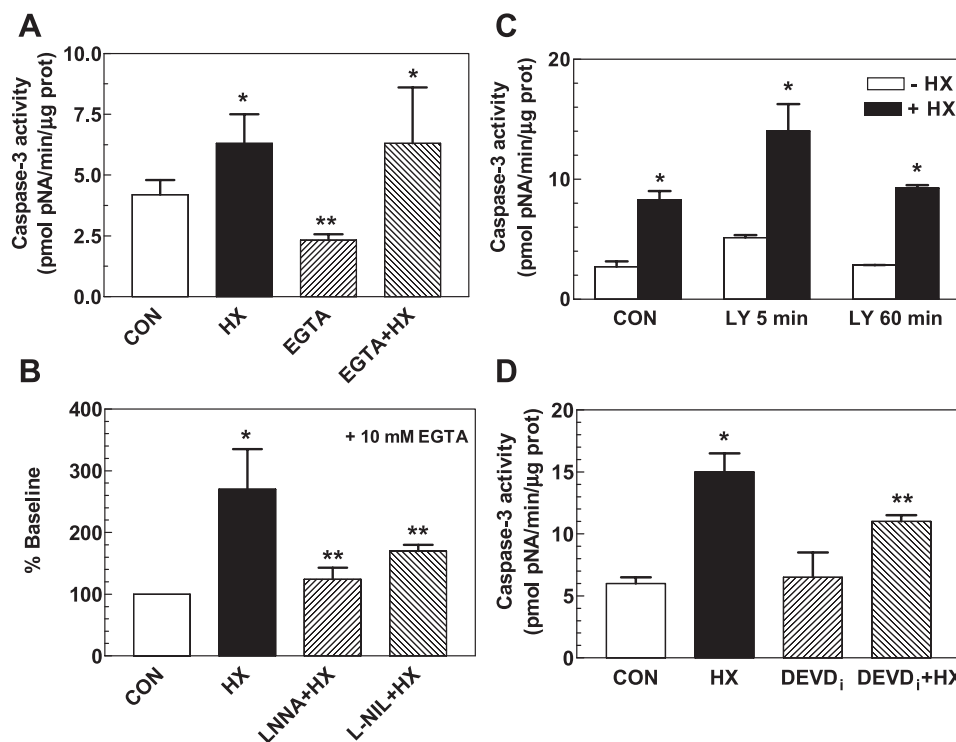
Fig. 6. Hypoxia-induced increases in caspase-3 are inhibited by iNOS inhibitor but not by removal of external Ca^{2+} or PI3K/Akt pathway in intestinal cells. *A*: to stimulate hypoxia (HX), intestinal epithelial cells were exposed to 10 mM NaCN for 1 h in Na^+ Hanks' buffer with 1.6 mM Ca^{2+} or Ca^{2+}-free Na^+ Hanks' buffer containing 3 mM EGTA. Removal of external Ca^{2+} failed to inhibit the HX-induced increases in caspase-3 activity. *$P < 0.05$ vs. control group and EGTA group, **$P < 0.05$ vs. control, HX, and EGTA+HX, determined by χ^2 test. *B*: cells were treated with 100 μM L-NNA or L-NIL in absence of external Ca^{2+} for 30 min prior to exposure to 10 mM NaCN for 1 h. Both iNOS inhibitors effectively blocked HX-induced increases in caspase-3 activity. *$P < 0.05$ vs. control group, L-NNA+HX group, and L-NIL+HX group; **$P < 0.05$ vs. control group and HX group, determined by χ^2 test. *C*: cells were treated with 100 μM LY-29402 in presence of external Ca^{2+} for 5 or 60 min followed by exposure to 10 mM NaCN for 1 h. LY-29402 failed to inhibit the HX-induced increase in caspase-3 activity. *$P < 0.05$ vs. respective control group, determined by Student's *t*-test. *D*: cells were treated for 16 h with 150 μM DEVD inhibitor (DEVDi) prior to exposure to 10 mM NaCN for 1 h. *$P < 0.05$ vs. control, DEVDi-treated, and DEVDi+HX groups; **$P < 0.05$ vs. control, HX, and DEVDi-treated groups, determined by χ^2 test.

organ-specific differences in how the drug interacts with the tissues.

We investigated the cause of the increased caspase-3 activity. Figure 3 clearly demonstrates that hemorrhage elevates the amount of caspase-3 protein in mouse jejunum. Most likely, the increased amount of caspase-3 protein accounts for the elevated caspase-3 activity observed after hemorrhage. Figure 3 also shows that the inhibition of caspase-3 by GA appears to be the result of an inhibition of the hemorrhage-induced increase in caspase-3 protein. Interventions that lead to inhibition of caspase-3 activity (45) such as treadmill exercise (26), hypertonic saline resuscitation (31), lactated Ringer resuscitation (19), or treatment with 5-androstenediol (20) have been shown to reduce tissue apoptosis and brain damage in hemorrhaged animals. Our results with GA are consistent with these reports.

Stimulated increases in caspase-3 activity in the cell can occur through a variety of mechanisms, including activation of the PI3K/Akt pathway. Using cultured cells exposed to hypoxia, a model for hemorrhage in animals, we tested whether this process plays a role in increasing caspase-3 activity. The pathway inhibitor LY29402 failed to block caspase-3 stimulation, indicating the PI3K/Akt pathway plays no role in the stimulation we observed (Fig. 6B). We also determined that calcium influx is not involved in the hypoxia-induced increase in caspase-3 because experiments

showing that incubating cells in medium containing EGTA had no effect (Fig. 6A). Interestingly, however, we found that the iNOS inhibitors L-NNA and L-NIL both inhibited the caspase-3 increase following hypoxia (even in the absence of extracellular calcium; Fig. 6C). A similar result was previously shown with the iNOS inhibitor 5-androstenediol (20).

These results clearly implicate iNOS as having a role in the activation of caspase-3 after hypoxia (and therefore hemorrhage). We and other laboratories reported that hemorrhage increases iNOS expression (11, 17, 23, 30, 34) by upregulating its transcriptional factors (15, 17, 19, 23). As a result of the increased iNOS expression (23, 38, 39), NO production increases, which leads to nitrosative stress and the release of cytochrome c from the mitochondria to the cytosol (2, 11, 12, 25, 36). The cytosolic cytochrome c then associates with caspase-9 and Apaf-1 to form the apoptosomes (Fig. 4), which is directly responsible for triggering caspase-3 activity (13, 14, 22) and apoptosis.

The view that iNOS activates caspase-3 activity is further supported by our experiments in which we manipulated the gene expression of iNOS to determine the effect on caspase-3 activity. Forced overexpression of iNOS leads to an increase in caspase-3 protein (Fig. 7A) and therefore its total enzymatic activity. Consistent with this observation, treatment with iNOS siRNA, which silenced iNOS protein expression, led to a
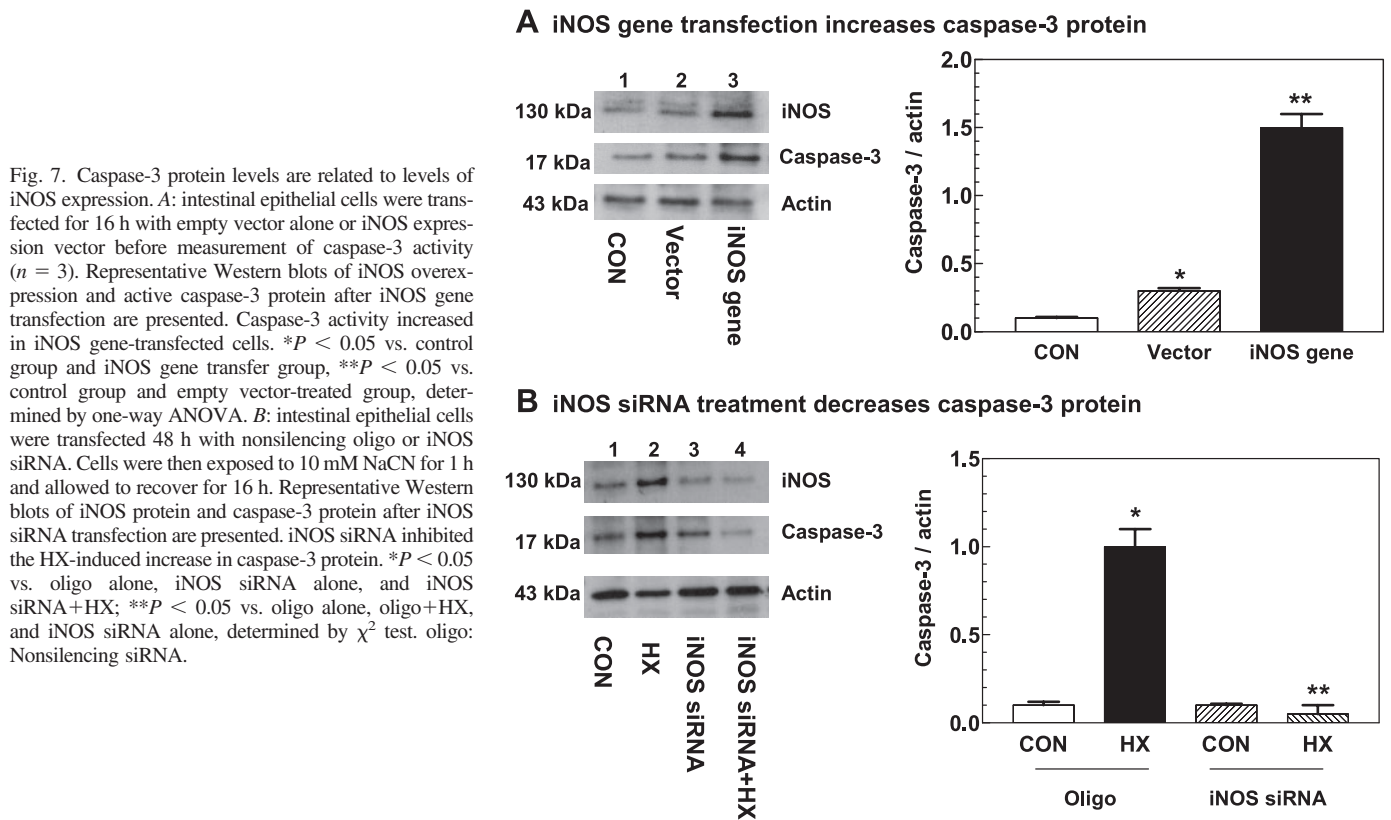
A iNOS gene transfection increases caspase-3 protein

Fig. 7. Caspase-3 protein levels are related to levels of iNOS expression. *A*: intestinal epithelial cells were transfected for 16 h with empty vector alone or iNOS expression vector before measurement of caspase-3 activity ($n = 3$). Representative Western blots of iNOS overexpression and active caspase-3 protein after iNOS gene transfection are presented. Caspase-3 activity increased in iNOS gene-transfected cells. $*P < 0.05$ vs. control group and iNOS gene transfer group, $**P < 0.05$ vs. control group and empty vector-treated group, determined by one-way ANOVA. *B*: intestinal epithelial cells were transfected 48 h with nonsilencing oligo or iNOS siRNA. Cells were then exposed to 10 mM NaCN for 1 h and allowed to recover for 16 h. Representative Western blots of iNOS protein and caspase-3 protein after iNOS siRNA transfection are presented. iNOS siRNA inhibited the HX-induced increase in caspase-3 protein. $*P < 0.05$ vs. oligo alone, iNOS siRNA alone, and iNOS siRNA+HX; $**P < 0.05$ vs. oligo alone, oligo+HX, and iNOS siRNA alone, determined by χ^2 test. oligo: Nonsilencing siRNA.

B iNOS siRNA treatment decreases caspase-3 protein

decrease in caspase-3 enzymatic activity and protein expression (Fig. 7*B*). Additional support for the idea that iNOS regulates caspase-3 comes with our observation of an increase in cytosolic cytochrome c in iNOS gene-transfected cells.

Cytochrome c complexed caspase-9 and Apaf-1 to form apoptosomes (Fig. 8). Conversely, downregulation of iNOS interfered with apoptosomes complex formation and caspase-3 activity (Fig. 9).
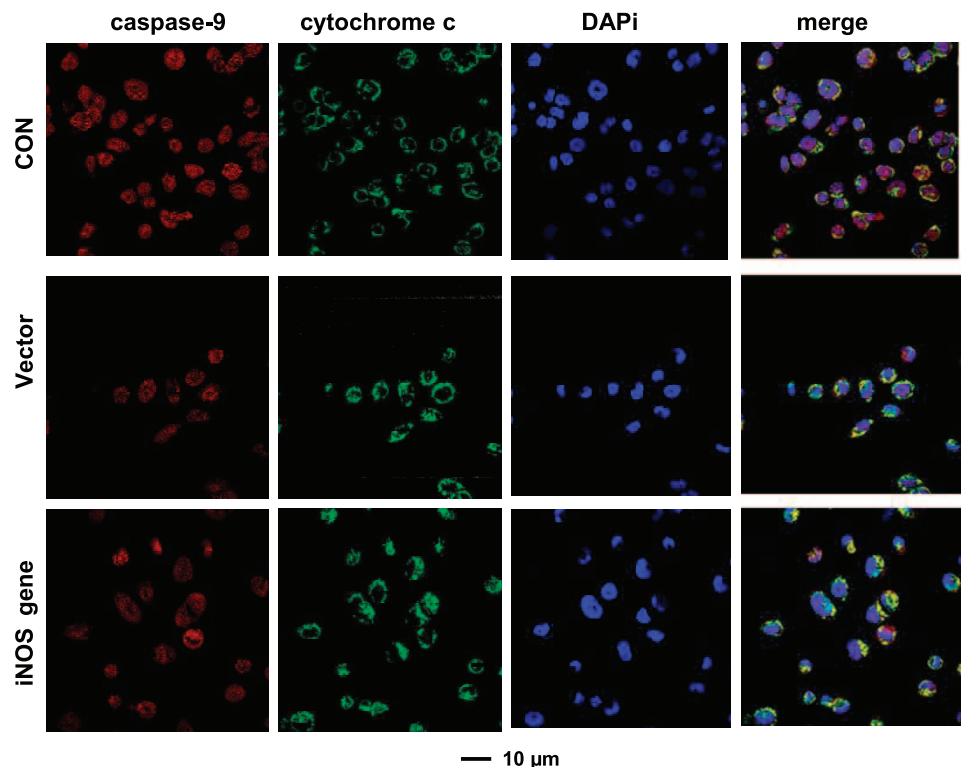

Fig. 8. iNOS overexpression leads to increases in formation of caspase-9-cytochrome c complex. Intestinal epithelial cells were transfected for 16 h with empty vector alone or iNOS expression vector ($n = 3$). Cells were stained immunofluorescently with antibodies directed against caspase-9 (red), cytochrome c (green), or DAPI (blue). Merged images depict colocalization of caspase-9 and cytochrome c (yellow).
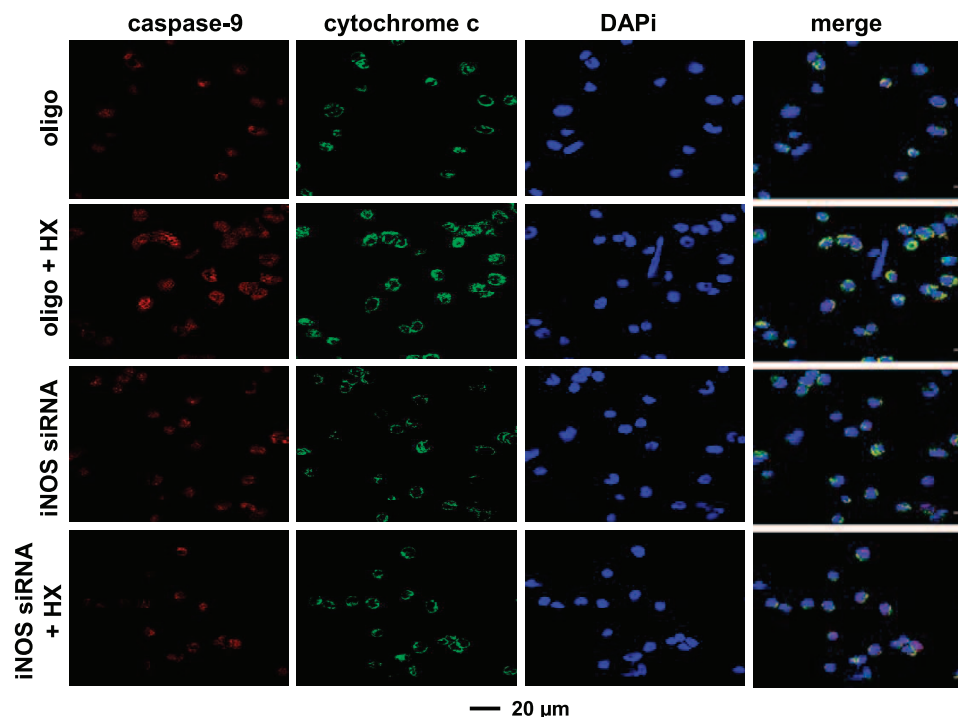
Fig. 9. iNOS inhibition leads to reduction of caspase-9-cytochrome c complex. Intestinal epithelial cells were transfected for 48 h with nonsilencing oligo or iNOS siRNA. Cells were then exposed to 10 mM NaCN for 1 h and allowed to recover for 16 h ($n = 3$). Treated cells were stained immunofluorescently with antibodies directed against caspase-9 (red), cytochrome c (green), or DAPI (blue). Merged images depict colocalization of caspase-9 and cytochrome c (yellow).

It has been shown that treatment of cells (23) or animals (17) with iNOS inhibitors results in decreased cellular caspase-3 activity and increased survival. In previous studies, we determined that GA inhibits iNOS by regulating the iNOS transcriptional factors (16). In the present study, GA inhibited apoptosomes formation in hemorrhaged jejunum (Fig. 4) and prevented intestinal mucosal and pulmonary injury in mice following hemorrhage (Fig. 5).

The full mechanisms of the hemorrhage-associated maladies MOD and MOF are not yet clear. It is interesting to note that the time course data we showed for the increase in caspase-3 activity following hemorrhage are generally consistent with the development of the symptoms MOD and MOF in both mice

and humans (3, 7–9, 37, 44). That is, our data show an early and continuous increase in caspase-3 activity in lung, an initial increase followed by a second increase in kidney, and a delayed increase in brain. Additional studies of this relationship could prove to be useful. The GA-mediated inhibition of increases in the caspase-3 activity and its ability to limit intestinal mucosal and pulmonary injury following hemorrhage may make GA a useful therapeutic agent to decrease MOD and MOF after hemorrhage.

The potential therapeutic benefit of GA is further supported by the following facts. First, GA inhibits KLF6 expression activated by hemorrhage (17, 18) or wound repair (35). Second, GA inhibits hemorrhage-induced iNOS overexpression,
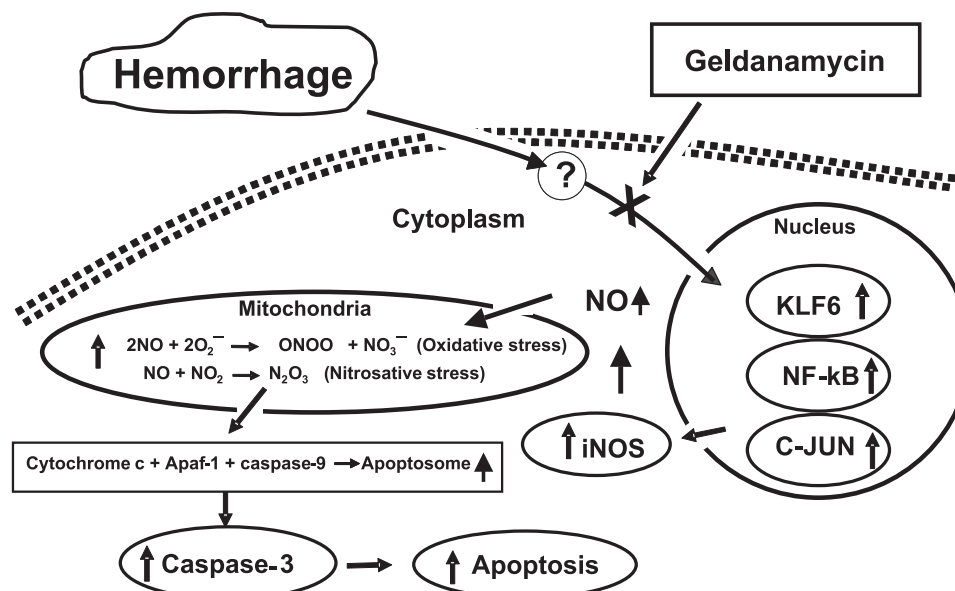

Fig. 10. Schematic representation of model for caspase-3 activity after hemorrhage and site of GA action. Hemorrhage, through poorly understood events, triggers increases in c-jun, Kruppel-like factor 6 (KLF6) and NF-κB 50 kDa that lead to iNOS activity increase (17). Increase in iNOS activity leads to increase in NO (39), which reacts with NO_2 to form N_2O_3, creating nitrosative stress. NO also reacts with O_2^- to form $OONO^-$, and NO_3^-, creating oxidative stress (42). Nitrosative and oxidative stress leads to rupture of mitochondria and release of cytochrome c into cytoplasm. Cytoplasmic cytochrome c is complexed by Apaf-1 and caspase-9 to form apoptosomes. Apoptosomes then activate caspase-3 and caspase-7 (13, 14, 22, 25), initiating cascade of reactions leading to cell death, which may explain MOF (3, 7–9, 37, 44). GA inhibits poorly understood events upstream from increases in c-jun, KLF6, and NF-κB 50 kDa. MOF, multiple organ failure.

which diminishes the iNOS-induced cell injury (11, 15, 17–19, 34). Third, GA treatment effectively decreases the hemorrhage-induced increase in key apoptotic proteases (Fig. 5). Finally, GA increases ATP levels (16). Thus it is reasonable to propose that GA would have therapeutic effects and it could be used to limit the acute and delayed injury resulting from hemorrhage.

Figure 10 presents a hypothetical model depicting the hemorrhage-induced changes in mouse jejunum consistent with our data, indicating the point where GA might be exerting its inhibitory effect. Hemorrhage, through signals not yet fully understood, increases c-jun, KLF6, and NF-κB 50 kDa, which stimulates increased iNOS activity. The increase in iNOS leads to increased levels of NO in the cytoplasm, which then reacts with NO_2 in the mitochondria to form N_2O_3, thereby triggering nitrosative stress. NO also reacts with O_2^- to form $OONO^-$ and NO_3^-, thereby triggering oxidative stress. In addition, NO reacts with biological metals, modulating catalase and GSH, and thereby further altering cell sensitivity to cell death (42). Nitrosative stress and oxidative stress are known to rupture mitochondria, which results in a release of cytochrome c that complexes with cytosolic Apaf-1 and caspase-9 to form apoptosomes. Apoptosomes activate caspase-3 and caspase-7 (13, 14, 22, 25), switching on the cascade of reactions that lead to apoptosis and possibly, MOF (3, 7–9, 37, 44). Our previous experiments have shown that GA inhibits the hemorrhage-induced increases in c-jun, KLF6, and NFκB 50 kDa (16). GA inhibition may occur upstream of its effect on these transcription factors, but those upstream events are not yet understood. By blocking those events, GA ultimately blocks the reactions that lead to apoptosis.

In summary, we showed that hemorrhage induces an increase in the amount of caspase-3 protein in the cell, which results in increased caspase-3 activity. We demonstrated that GA treatment decreases the caspase-3 response to hemorrhage by inhibiting the iNOS pathway, which results in a reduction in apoptosome formation and thus, apoptosis. Further research is required to understand the specific site of GA action in this process. Our results suggest that GA may have therapeutic value in preventing tissue damage associated with hemorrhage, possibly used as an adjuvant in resuscitation fluids to resuscitate patients with blood loss.

REFERENCES

1. **Baue AE, Durham R, Faist E.** Systemic inflammatory response syndrome (MODS), multiple organ dysfunction syndrome (MODS), multiple organ failure (MOF): are we winning the battle? *Shock* 10: 79–89, 1998.
2. **Brown GC.** Nitric oxide and mitochondria. *Front Biosci* 12: 1024–1033, 2007.
3. **Caruso JM, Feketeova E, Dayal SD, Hauser CJ, Deitch EA.** Gut injury and gut-induced lung injury after trauma hemorrhagic shock is gender and estrus cycle specific in the rat. *J Trauma* 55: 531–539, 2003.
4. **Chiu CJ, McArdle AH, Brown R, Scott HJ, Gurd FN.** Intestinal mucosal lesion in low-flow states: a morphological, hemodynamic and metabolic reappraisal. *Arch Surg* 101: 478–483, 1970.
5. **Cho NH, Lee JD, Cheong BS, Choi DY, Chang HK, Lee TH, Shin MC, Shin MS, Lee J, Kim CJ.** Acupuncture suppresses intrastriatal hemorrhage-induced apoptotic neuronal cell death in rats. *Neurosci Lett* 362: 141–145, 2004.
6. **Conde AG, Lau SS, Dillmann WH, Mestril R.** Induction of heat shock proteins by tyrosine kinase inhibitors in rat cardiomyocytes and myogenic cells confers protection against simulated ischemia. *J Mol Cell Cardiol* 29: 1927–1938, 1997.
7. **Davidson MT, Deitch EA, Lu Q, Hasko G, Abungu B, Nemeth ZH, Zaets SB, Gaspers LD, Thomas AP, Xu DZ.** Trauma-hemorrhagic shock mesenteric lymph induces endothelial apoptosis that involves both caspase-dependent and caspase-independent mechanisms. *Ann Surg* 240: 123–131, 2004.
8. **Deitch EA, Xu D, Kaise VL.** Role of the gut in the development of injury- and shock induced SIRS and MODS: the gut-lymph hypothesis, a review. *Front Biosci* 11: 520–528, 2006.
9. **Deitch EA.** Role of the gut lymphatic system in multiple organ failure. *Curr Opin Crit Care* 7: 92–98, 2001.
10. **Ghosh DK, Rashid MB, Crane B, Taskar V, Mast M, Misukonis MA, Weinberg JB, Eissa NT.** Characterization of key residues in the subdomain encoded by exon 8 and 9 of human inducible nitric oxide synthase: a critical role for Asp-280 in substrate binding and subunit interactions. *Proc Natl Acad Sci USA* 98: 10392–10397, 2001.
11. **Hierholzer C, Harbrecht B, Menezes JM, Kane J, MacMicking J, Nathan CF.** Essential role of induced nitric oxide in the initiation of the inflammatory responses after hemorrhagic shock. *J Exp Med* 187: 917–928, 1998.
12. **Hierholzer C, Kalff JC, Billiar TR, Bauer AJ, Tweardy DJ, Harbrecht BG.** Induced nitric oxide promotes intestinal inflammation following hemorrhagic shock. *Am J Physiol Gastrointest Liver Physiol* 286: G225–G233, 2004.
13. **Hill MM, Adrain C, Martin SJ.** Portrait of a killer: the mitochondrial apoptosome emerges from the shadow. *Mol Interventions* 3: 19–25, 2003.
14. **Jiang X, Wang X.** Cytochrome-c-mediated apoptosis. *Annu Rev Biochem* 73: 87–106, 2004.
15. **Kiang JG.** Inducible heat shock protein 70 kD and inducible nitric oxide synthase in hemorrhage/resuscitation-induced injury. *Cell Res* 14: 450–459, 2004.
16. **Kiang JG, Bowman DP, Lu X, Li Y, Ding XZ, Zhao B, Juang YT, Atkins JL, Tsokos GC.** Geldanamycin treatment prevents hemorrhage-induced ATP loss by overexpressing HSP-70 and activating pyruvate dehydrogenase. *Am J Physiol Gastrointest Liver Physiol* 291: G117–G127, 2006.
17. **Kiang JG, Bowman PD, Wu BW, Hampton N, Kiang AG, Zhao B, Juang YT, Atkins JL, Tsokos GC.** Geldanamycin treatment inhibits hemorrhage-induced increases in KLF6 and iNOS expression in unresuscitated mouse organs: role of inducible HSP-70. *J Appl Physiol* 97: 564–569, 2004.
18. **Kiang JG, Bowman PD, Wu BW, Hampton N, Kiang AG, Zhao B, Juang YT, Atkins JL, Tsokos GC.** Geldanamycin inhibits hemorrhage-induced increases in caspase-3 activity, KLF6 and iNOS expression in unresuscitated organs of mice: role of inducible HSP-70. *FASEB J* 18: A220–A221, 2004.
19. **Kiang JG, Lu X, Tabaku LS, Bentley TB, Atkins JL, Tsokos GC.** Resuscitation with lactated Ringer's solution limits the expression of molecular events associated with lung injury after hemorrhage. *J Appl Physiol* 98: 550–556, 2005.
20. **Kiang JG, Peckham RM, Duke LE, Shimizu T, Chaudry IH, Tsokos GC.** Androstenediol inhibits the trauma-hemorrhage-induced increase in caspase-3 by downregulating the inducible nitric oxide synthase pathway. *J Appl Physiol* 102: 933–941, 2007.
21. **Kiang JG, Smallridge RC.** Sodium cyanide increases cytosolic free calcium: evidence of activation of the reversed mode of Na^+/Ca^{2+} exchanger and Ca^{2+} mobilization from inositol trisphosphate-insensitive pools. *Toxicol Appl Pharmacol* 127: 173–181, 1994.
22. **Kiang JG, Tsen KT.** Biology of hypoxia. *Chin J Physiol* 49: 223–233, 2006.

23. **Kiang JG, Warke VG, Tsokos GC.** NaCN-induced chemical hypoxia is associated with altered gene expression. *Mol Cell Biochem* 254: 211–216, 2003.

24. **Kline JA, Maiorano PC, Schroeder JD, Grattan RM, Vary TC, Watts JA.** Activation of pyruvate dehydrogenase improves heart function and metabolism after hemorrhagic shock. *J Mol Cell Cardiol* 29: 2465–2474, 1997.

25. **Lakhani SA, Masud A, Kuida K, Porter GA Jr, Booth CJ, Mehal WZ, Inayat I, Flavell RA.** Caspases 3 and 7: key mediators of mitochondrial events of apoptosis. *Science* 311: 847–51, 2006.

26. **Lee HH, Kim H, Lee MH, Chang HK, Lee TH, Jang MH, Shin MC, Lim BV, Shin MS, Kim YP, Yoon JH, Jeong IG, Kim CJ.** Treadmill exercise decreases intrastriatal hemorrhage-induced neuronal cell death via suppression on caspase-3 expression in rats. *Neurosci Lett* 352: 33–36, 2003.

27. **Mauriz JL, Gonzalez P, Jorquera F, Olcoz JL, Gonzalez-Gallego J.** Caspase inhibition does not protect against liver damage in hemorrhagic shock. *Shock* 19: 33–37, 2003.

28. **Mizushima Y, Wang P, Jarrar D, Cioffi WG, Bland KI, Chaudry IH.** Preinduction of heat shock proteins protects cardiac and hepatic functions following trauma and hemorrhage. *Am J Physiol Regul Integr Comp Physiol* 278: R352–R359, 2000.

29. **Mongan PD, Capacchione J, West S, Karaian J, Dubois D, Keneally R, Sharma P.** Pyruvate improves redox status and decreases indicators of hepatic apoptosis during hemorrhagic shock in swine. *Am J Physiol Heart Circ Physiol* 283: H1634–H1644, 2002.

30. **Moore WM, Webber RK, Jerome GM, Tjoeng FS, Misko TP, Currie MG.** L-N⁶-(1-iminoethyl)lysine: a selective inhibitor of inducible nitric oxide synthase. *J Med Chem* 37: 3886–3888, 1994.

31. **Murao Y, Hata M, Ohnishi K, Okuchi K, Nakajima Y, Hiasa Y, Junger WG, Hoyt DB, Ohnishi T.** Hypertonic saline resuscitation reduces apoptosis and tissue damage of the small intestine in a mouse model of hemorrhagic shock. *Shock* 20: 23–28, 2003.

32. **Paxian M, Bauer I, Rensing H, Jaeschke H, Mautes AE, Kolb SA, Wolf B, Stockhausen A, Jeblick S, Bauer M.** Recovery of hepatocellular ATP and "pericentral apoptosis" after hemorrhage and resuscitation. *FASEB J* 17: 993–1002, 2003.

33. **Pearce FJ, Connett RJ, Drucker WR.** Phase-related changes in tissue energy reserves during hemorrhagic shock. *J Surg Res* 39: 390–398, 1985.

34. **Pittet JF, Lu LN, Geiser T, Lee H, Matthay A, Welch WJ.** Stress preconditioning attenuates oxidative injury to the alveolar epithelium of the lung following haemorrhage in rats. *J Physiol* 538: 583–597, 2001.

35. **Ratziu V, Lalazar A, Wong L, Dang Q, Collins C, Shaulian E, Jensen S, Friedman SL.** Zf9, a Kruppel-like transcription factor up-regulated in vivo during early hepatic fibrosis. *Proc Natl Acad Sci USA* 95: 9500–9505, 1998.

36. **Ryter SW, Kim HP, Hoetzel A, Park JW, Nakahira K, Wang X, Choi AM.** Mechanisms of cell death in oxidative stress. *Antioxid Redox Signal* 9: 49–89, 2007.

37. **Senthil M, Brown M, Xu DZ, Lu Q, Feketeova E, Deitch EA.** Gut-lymph hypothesis of systemic inflammatory response syndrome/multiple-organ dysfunction syndrome: validating studies in a porcine model. *J Trauma* 60: 958–967, 2006.

38. **Shea-Donohue T, Anderson J, Swiecki C.** Ischemia/reperfusion injury. In: *Combat Medicine—Basic and Clinical Research in Military, Trauma, and Emergency Medicine*, edited by Tsokos GC and Atkins JL). New Jersey: Humana, 2003, p. 219–248.

39. **Shimizu T, Szalay L, Choudhry MA, Schwacha MG, Rue LWIII, Bland KI, Chaudry IH.** Mechanism of salutary effects of androstenediol on hepatic function following trauma-hemorrhage: the role of endothelin 1 and inducible nitric oxide synthase. *Am J Physiol Gastrointest Liver Physiol* 288: G244–G250, 2005.

40. **Song Y, Ao L, Raeburn CD, Calkins CM, Abraham E, Harken AH, Meng X.** A low level of TNF-α mediates hemorrhage-induced acute lung injury via p55 TNF receptor. *Am J Physiol Lung Cell Mol Physiol* 281: L677–L684, 2001.

41. **Stojadinovic A, Kiang JG, Smallridge RC, Galloway RL, Shea-Donahue T.** *H*eat shock protein 72 kD induction protects rat intestinal mucosa from ischemia/reperfusion injury. *Gastroenterology* 109: 505–515, 1995.

42. **Thomas DD, Miranda KM, Citrin D, Espey MG, Wink DA.** Nitric oxide. In: Combat Medicine—Basic and Clinical Research in Military, Trauma, and Emergency Medicine, edited by Tsokos GC and Atkins JL. New Jersey: Humana, 2003, p. 23–60.

43. **Van Way CW 3rd, Dhar A, Morrison DC, Longorio MA, Maxfield DM.** Cellular energetics in hemorrhagic shock: restoring adenosine triphosphate to the cells. *J Trauma* 54: S169–S176, 2003.

44. **Xu DZ, Lu Q, Deitch EA.** Nitric oxide directly impairs intestinal barrier function. *Shock* 17: 139–145, 2002.

45. **Zhou C, Yamaguchi M, Kusaka G, Schonholz C, Nanda A, Zhang JH.** Caspase inhibitors prevent endothelial apoptosis and cerebral vasospasm in dog model of experimental subarachnoid hemorrhage. *J Cereb Blood Flow Metab* 24: 419–431, 2004.